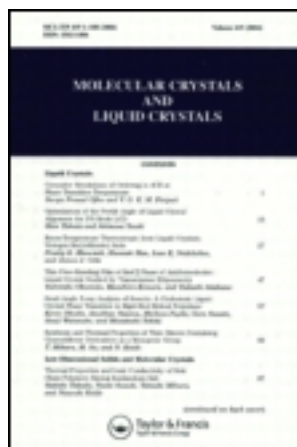


This article was downloaded by: [Tomsk State University of Control Systems and Radio]
On: 23 February 2013, At: 03:13
Publisher: Taylor & Francis
Informa Ltd Registered in England and Wales Registered Number: 1072954 Registered office: Mortimer House, 37-41 Mortimer Street, London W1T 3JH, UK



Molecular Crystals and Liquid Crystals

Publication details, including instructions for authors and subscription information:

<http://www.tandfonline.com/loi/gmcl16>

Physicochemical Study on Liquid Crystal-Substrate Interfacial Interactions

Shohei Naemura^a

^a Opto-Electronics Research Laboratories,
Nippon Electric Co., Ltd., 4-1-1 Miyazaki,
Takatsu-ku, Kawasaki, 213, Japan

Version of record first published: 14 Oct 2011.

To cite this article: Shohei Naemura (1981): Physicochemical Study on Liquid Crystal-Substrate Interfacial Interactions, *Molecular Crystals and Liquid Crystals*, 68:1, 183-198

To link to this article: <http://dx.doi.org/10.1080/00268948108073563>

PLEASE SCROLL DOWN FOR ARTICLE

Full terms and conditions of use: <http://www.tandfonline.com/page/terms-and-conditions>

This article may be used for research, teaching, and private study purposes. Any substantial or systematic reproduction, redistribution, reselling, loan, sub-licensing, systematic supply, or distribution in any form to anyone is expressly forbidden.

The publisher does not give any warranty express or implied or make any representation that the contents will be complete or accurate or up to date. The accuracy of any instructions, formulae, and drug doses should be independently verified with primary sources. The publisher shall not be liable for any loss, actions, claims, proceedings, demand, or

costs or damages whatsoever or howsoever caused arising directly or indirectly in connection with or arising out of the use of this material.

Physicochemical Study on Liquid Crystal-Substrate Interfacial Interactions†

SHOHEI NAEMURA

*Opto-Electronics Research Laboratories, Nippon Electric Co., Ltd.
4-1-1 Miyazaki, Takatsu-ku, Kawasaki 213, Japan*

(Received August 4, 1980)

Surface energies and liquid crystal MBBA orientations were investigated on substrates with organic layers. Polar and nonpolar contributions to the MBBA interfacial orientations were explained in terms of the chemical structures of the organic layers. Numerical calculations clearly showed that the liquid crystal interfacial orientation conditions are subject to liquid crystal and substrate surface energy differences in both polar and nonpolar components. Calculations agree well with the measured results on both MBBA orientation angles and anchoring strengths at the organic layer surfaces.

1 INTRODUCTION

Liquid crystal (LC) molecular orientation in a bulk can be controlled by controlling the orientation on a substrate surface. As the LC orientation control is particularly important for LC devices, many efforts have been made both to develop techniques for orienting LC molecules and to study their mechanisms.

Various techniques for controlling the LC orientation angles have been developed, including rubbing,¹ oblique evaporation^{2,3} and organic film formation.^{4,5} Equilibrium orientation distribution of LC molecules in a bulk as the result of the surface treatment corresponds to the condition which minimizes the total energy including the elastic deformation energy and the interfacial interaction energy. For the director elastic deformation energies, the continuum theory successfully explained the molecular orienting effects of surface microgrooves.⁶ Besides the bulk elastic deformation forces, the inter-

† Presented at the Eighth International Liquid Crystal Conference in Kyoto, June 30-July 4, 1980.

molecular interactions at the substrate surface play important roles, especially in the case of flat surfaces. Several studies have been directed to explain the correlations between LC molecular orientation and the substrate surface energies. Pioneer works in this field were made by Creagh-Kmetz⁷ and Kahn,⁸ who stated that the homeotropic orientation is produced by substrates whose critical surface tension γ_c is smaller than LC surface tensions. However, this γ_c -hypothesis lacks universal validity.⁹ Perez *et al.*¹⁰ insisted on the necessity for considering polar interaction contributions. Recently, the author¹¹ presented clear evidence on polar and dispersive force contributions to LC molecular orientations on substrates, and clarified that the γ_c -hypothesis is valid only when polar interfacial interactions are negligible.

At an earlier stage, the interfacial interaction forces were assumed to be large enough for restricting LC molecular orientation in the "easy axis" direction against external fields which act to reorient LC molecules. However, some topological observations^{12,13} and measurements on director deformation under a magnetic field¹⁴ suggest that interfacial interaction forces between LC molecules and substrate surfaces with organic layers are usually not so strong. The weak anchoring conditions were observed for various substrate surfaces with surfactant layers.¹⁵ It was also reported that the surface anchoring strength affects LC display devices characteristics.^{16,17} For manufacturing LC display devices with desired characteristics, therefore, it is necessary to control not only LC molecular orientation angle but also LC molecular anchoring strength on substrate surfaces. For this purpose, it is strongly required to clarify the LC molecular orientation mechanisms on substrates.

This paper aims to clarify polar and dispersive force contributions to LC molecular orientations on substrates, especially those which are coated with organic layers. The surface orientation of nematic LC molecules is characterized using orientation angles (θ_0 , ϕ_0) and anchoring strength coefficient (B_θ , B_ϕ).¹⁵ Section 2 describes the calculated results concerning correlations between the interfacial orientation parameters (θ , B_θ) and the polar and dispersive components (γ_s^p , γ_s^d) for substrate surface energies. Section 3 presents the method for measuring (θ_0 , B_θ) and (γ_s^p , γ_s^d) and experimental results on the correlations between them. Section 4 gives a discussion on the causes producing the (γ_s^p , γ_s^d) differences for the measured substrate surfaces. Section 5 presents some concluding remarks.

2 CALCULATIONS FOR LC ORIENTATION PARAMETERS

2.1 Interfacial interaction energy representation

The LC molecular orientation has to minimize the total free energy,

$$F = \int W_L dV + \int W_{SL} dS, \quad (1)$$

where W_L is the free energy per unit volume and W_{SL} is the interfacial free energy per unit area. In this paper, we consider the case when no orientational distributions exist at the interface. In such a case, no orientational deformations exist in the LC bulk, and the equilibrium LC orientation is determined by minimizing W_{SL} instead of F . Moreover, by choosing the coordinates system to satisfy ϕ_0 (the director azimuthal angle) $= 0^\circ$, W_{SL} is represented as a single variable function of θ_0 , the director polar angle. In the following, therefore, we consider the interfacial energy density $W_{SL}(\theta_0)$ instead of the total free energy F . W_{SL} is represented as

$$W_{SL} = \gamma_s + \gamma_{LC} - W_a, \quad (2)$$

by using substrate surface energy γ_s , LC surface energy γ_{LC} and work of adhesion W_a needed to separate the LC bulk infinitely from the substrate surface. We assume that each term in Eq. (2) is sum of dispersive and polar force components, whose origins are independent from each other,

$$\begin{aligned} \gamma_s &= \gamma_s^d + \gamma_s^p, \\ \gamma_{LC} &= \gamma_{LC}^d + \gamma_{LC}^p, \\ W_a &= W_a^d + W_a^p, \end{aligned} \quad (3)$$

where superscripts d and p represent dispersive and polar components, respectively.

Dispersive terms in W_{SL} According to Fowkes,¹⁸ W_{SL} is given by a formula,

$$W_a^d = 2\{\gamma_s^d \cdot \gamma_{LC}^d(\theta)\}^{1/2}. \quad (4)$$

Therefore, the dispersive term of $W_{SL}(\theta)$ becomes

$$\begin{aligned} W_{SL}^d(\theta) &= \gamma_s^d + \gamma_{LC}^d(\theta) - W_a^d \\ &= \{\gamma_s^{d/2} - \gamma_{LC}^d(\theta)^{1/2}\}^2. \end{aligned} \quad (5)$$

γ_{LC}^d originates from the London–Van der Waals force. Parsons¹⁹ derived a formula,

$$\gamma_{LC}^d = \gamma_1^d(S) + \gamma_2^d(S)(\mathbf{n} \cdot \mathbf{k})^2, \quad (6)$$

where S is the scalar order parameter, \mathbf{n} the director and \mathbf{k} the surface normal. As long as we are concerned in the LC orientation angle dependence of the interfacial energy, it is possible to consider that $\gamma_1^d(S)$ and $\gamma_2^d(S)$ are constant. Therefore, γ_{LC}^d is represented in the form of Eq. (6) as

$$\gamma_{LC}^d(\theta) = \gamma_{LC}^d + \Delta \gamma_L^d \sin^2 \theta. \quad (7)$$

Polar terms in W_{SL} According to Girifalco,²⁰ the work of adhesion between semi-infinite volumes of i - and j -molecules is given by

$$W_{aj} = \left(\frac{n_i n_j A_{ij}}{6d_{ij}^2} \right) \left\{ \frac{1}{2} - \frac{1}{(m-4)} \right\}, \quad (8)$$

where n_i and n_j are molecular volume densities, d is the equilibrium separation between the volumes of i - and j -molecules, A_{ij} is an attraction constant and m is the repulsive exponent in the Lennard-Jones potential function. The Debye-Keesom theory gives a formulation for A_{ij} caused by the dipole-dipole interactions,

$$A_{ij}^P = \frac{2\mu_i^2 \mu_j^2}{3kT}. \quad (9)$$

Here, μ is the permanent dipole moment, k is the Boltzmann constant and T is the temperature. Similarly, the work of cohesion W_c is given by

$$W_{cii} = \left(\frac{n_i^2 A_{ii}}{6d_{ii}^2} \right) \left\{ \frac{1}{2} - \frac{1}{(m-4)} \right\}, \quad (10)$$

and

$$A_{ij}^P = 2\mu_i^4 / 3kT. \quad (11)$$

By assuming

$$d_{ij} = (d_{ii} d_{jj})^{1/2}, \quad (12)$$

Eqs. (8) ~ (11) lead to

$$W_{aj}^P = (W_{cii}^P W_{cij}^P)^{1/2}. \quad (13)$$

By considering

$$W_{cii}^P = 2\gamma_i^P, \quad (14)$$

we obtain

$$W_{aj}^P = 2(\gamma_i^P \gamma_j^P)^{1/2}. \quad (15)$$

By putting $i = S$ and $j = LC$, we have

$$W_a^P = 2\{\gamma_s^P \gamma_{LC}^P(\theta)\}^{1/2}. \quad (16)$$

Therefore, the polar term of $W_{SL}(\theta)$ becomes

$$\begin{aligned} W_{SL}^P(\theta) &= \gamma_s^P + \gamma_{LC}^P(\theta) - W_a^P \\ &= \{\gamma_s^{P1/2} - \gamma_{LC}^P(\theta)^{1/2}\}^2. \end{aligned} \quad (17)$$

The origins of polar forces are dipole-dipole interactions between permanent charge distributions, dipole-induced dipole interactions between a permanent

charge distribution and an induced moment, and bonding interactions, such as hydrogen bonding. The hydrogen bonding, however, is considered to be the electrostatic interaction between pertinent groups such as OH and NH. Since it is generally accepted that the dipole-dipole interaction is predominant for ordinary polar liquids, it is plausible to assume the dipole-dipole interaction is the dominant term in γ_{LC}^P . Parsons²¹ derived that $\gamma_{LC}^P(\theta)$ becomes minimum for $(\mathbf{n} \cdot \mathbf{k}) = 0$, when the permanent dipole is parallel to the molecular axis. By taking this result into consideration, it is possible to represent $\gamma_{LC}^P(\theta)$ in the similar form as Eq. (7) for $\gamma_{LC}^d(\theta)$. At the interface, however, there occurs the breakdown in LC molecular antiparallelism, which yields a linear term for $(\mathbf{n} \cdot \mathbf{k})$ in the $\gamma_{LC}^P(\theta)$ formula. In the bulk, the average S of quadrupole moment in the director direction is used as the LC order parameter, while the average P of dipole moment in the director direction becomes zero. On the contrary, the order parameter P should be taken into consideration for the dipole-dipole interaction at the interface, because P order exists ($P \neq 0$) close to the interface. Therefore, a pertinent formula is,

$$\gamma_{LC}^P = \gamma_1^P(S) + \gamma_2^P(S)(\mathbf{n} \cdot \mathbf{k})^2 + \gamma_3^P(P)(\mathbf{n} \cdot \mathbf{k}). \quad (18)$$

Equation (18) means that $(\mathbf{n} \cdot \mathbf{k}) = 0$ is not the solution for minimization condition, in contrast to the γ_{LC}^d term. For further calculations, it is convenient to represent γ_{LC}^P as a function of θ in the form of

$$\gamma_{LC}^P(\theta) = \gamma_{LO}^P + \Delta\gamma_L^P \sin^2(\theta - \Theta_P). \quad (19)$$

Here, Θ_P was introduced to represent the contribution of $\gamma_3^P(P)$ in Eq. (18). By adding $W_{SL}^d(\theta)$ and $W_{SL}^P(\theta)$, we have

$$W_{SL}(\theta) = \{\gamma_s^{d/2} - \gamma_{LC}^d(\theta)^{1/2}\}^2 + \{\gamma_s^{P/2} - \gamma_{LC}^P(\theta)^{1/2}\}^2, \quad (20)$$

where

$$\gamma_{LC}^d(\theta) = \gamma_{LO}^d + \Delta\gamma_L^d \sin^2\theta \text{ and } \gamma_{LC}^P(\theta) = \gamma_{LO}^P + \Delta\gamma_L^P \sin^2(\theta - \Theta_P).$$

2.2 Numerical calculations for LC orientations

Θ calculations For given values of substrate surface energies (γ_s^d, γ_s^P) and LC characteristic parameters ($\gamma_{LO}^d, \Delta\gamma_L^d, \gamma_{LO}^P, \Delta\gamma_L^P, \Theta_P$), it is possible to obtain the θ value which minimizes $W_{SL}(\theta)$, that is the easy axis angle Θ at the interface. The LC characteristic parameters are quite difficult to measure directly. For MBBA, however, dispersive and polar components of the surface energy are reported as $\gamma_{LO}^d = 29.0$ erg/cm² and $\gamma_{LO}^P = 9.0$ erg/cm².²² In addition, MBBA surface energy anisotropy is estimated to be 4.5×10^{-2} erg/cm².¹⁵ By taking these results into consideration, MBBA characteristic parameters were estimated as $(\gamma_{LO}^d, \Delta\gamma_L^d, \gamma_{LO}^P, \Delta\gamma_L^P) = (29.0, 4.5 \times 10^{-2}, 9.0, 4.5 \times 10^{-2})$. For Θ_P , $\Theta_P = 0^\circ$ was chosen to satisfy the measured homeotropic orientation tendency for MBBA at the free surface.

The relationships between Θ and γ_s^p for several γ_s^d values were calculated, as shown in Figure 1. Figure 1 shows that, in the case of $\gamma_s^d = 32.0 \text{ erg/cm}^2$ for example, $\gamma_s^p < 8 \text{ erg/cm}^2$ corresponds to the homeotropic ($\Theta = 0^\circ$) and $\gamma_s^p > 8 \text{ erg/cm}^2$ to the parallel ($\Theta = 90^\circ$) orientation. The upper limit of γ_s^p value for producing MBBA homeotropic orientation depends on γ_s^d value. The (γ_s^d, γ_s^p) region for MBBA homeotropic orientation is shown in Figure 2. According to the calculated results in Figure 2, it is possible to obtain MBBA homeotropic orientation by decreasing either polar or dispersive substrate surface energy component. These calculated results will be compared with the experimental results in Section 3.

B_θ calculations Anchoring strength at the interface, B_θ , is defined as an anisotropy coefficient in our model formula for the interfacial interaction energy,

$$W_{SL}(\theta_0) = \frac{A}{2} + \left(\frac{B_\theta}{2} \right) \sin^2(\theta_0 - \Theta). \quad (21)$$

In the case of $\Theta = 0^\circ$,

$$B_\theta = 2 \left\{ W_{SL} \left(\frac{\pi}{2} \right) - W_{SL}(0) \right\}. \quad (22)$$

Equation (22), together with Eq. (20), enables to calculate B_θ for given values of $(\gamma_{LO}^d, \Delta\gamma_L^d, \gamma_{LO}^p, \Delta\gamma_L^p, \theta_p)$ and (γ_s^d, γ_s^p) . Calculations were performed for MBBA by using the same characteristic parameter values as before. The re-

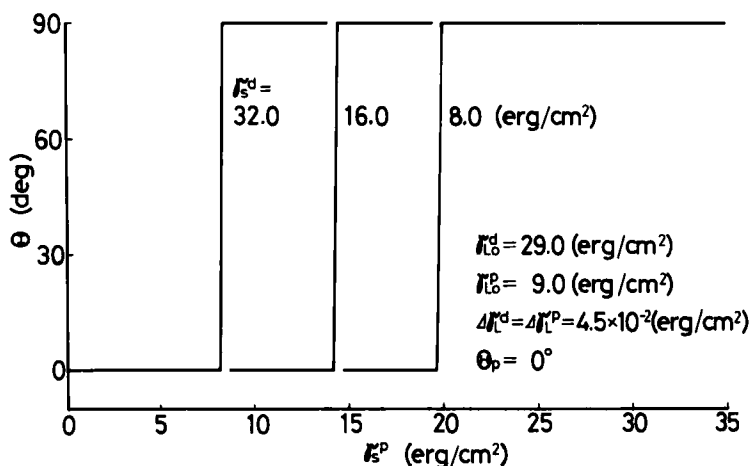


FIGURE 1 Calculated relationships between MBBA easy axis angle Θ and substrate polar surface energy γ_s^p ($\gamma_s^d = 8.0, 16.0, 32.0 \text{ erg/cm}^2$).

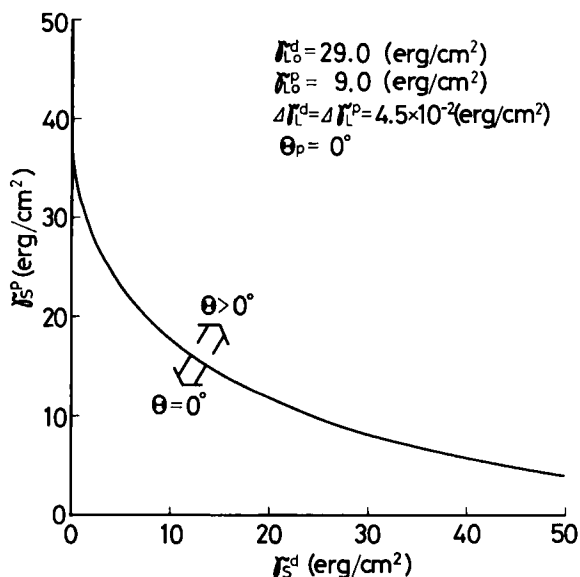


FIGURE 2 Calculated substrate surface energy condition for MBBA homeotropic orientation ($\theta = 0^\circ$).

sults are shown in Figure 3. According to Figure 3, stronger anchoring conditions are expected for MBBA on substrates with small surface energy components. These results are discussed in Section 3 in comparison with experimental results.

3 EXPERIMENTAL

Sample Preparations LC material used is *p*-methoxybenzylidene-*p*'-butylaniline (MBBA). Substrates used are glass plates, on which In_2O_3 was partly evaporated. The In_2O_3 evaporated areas were used for capacitance measurements. The substrates were coated with organic layers. The organic layer materials are cationic surfactants, coupling agents and resins, which are listed in Table I. Cationic surfactants are ammonium salts with alkyl chains (6Br and 8Br in Table I) and a perfluorocarbon chain (FS150). Their layers were deposited on the substrate surfaces from their solutions. The solvents are ethanol for 6Br and 8Br and water for FS150. Coupling agents are homologous series of silanes $n\text{S}$ ($n = 10, 12, 14, 16, 18$) and a chromium complex (Edran) with alkyl chains and another chromium complex (FC805) with a perfluorocarbon chain. Their layers were deposited using their aqueous solutions. In addition, silicone (SR2411), polyamide (Versamide 940) and poly-

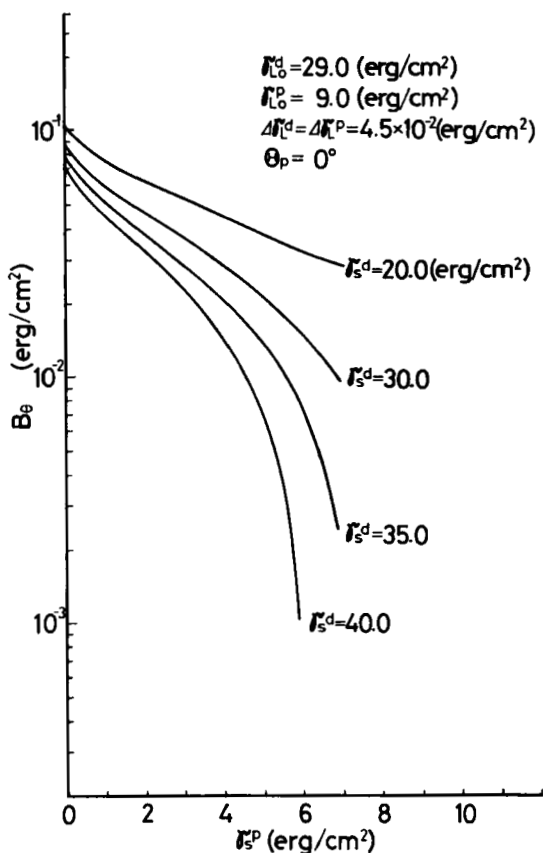


FIGURE 3 Calculated relationships between anchoring strength coefficients B_0 and substrate surface energy components (γ_s^d , γ_s^p)

imide (Toraynecce) resins were used. In case of the resins, the layers were formed by the spinner-coating method.

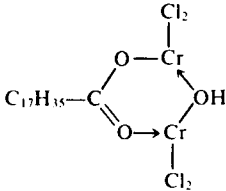
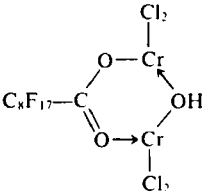
(γ_s^d , γ_s^p) derivations and θ_0 measurements for MBBA The substrate surface energy components (γ_s^d , γ_s^p) were derived by measuring advancing contact angles α of several liquids, including some polar liquids. The interfacial interaction energy W_{SL} for isotropic liquids is represented by

$$W_{SL} = \gamma_s + \gamma_L - 2\{(\gamma_s^d \gamma_L^d)^{1/2} + (\gamma_s^p \gamma_L^p)^{1/2}\}, \quad (23)$$

in a similar form to Eq. (20) for LCs. By combining Eq. (23) and the equation for correlating the interfacial interaction energy and the contact angle,

$$W_{SL} = \gamma_s - \gamma_L \cos \alpha, \quad (24)$$

TABLE I
 Examined organic layer materials.

Codes	Formulas
<i>Surfactants</i>	
6Br	$C_6H_{13}N^+(CH_3)_3Br^-$
8Br	$C_8H_{17}N^+(CH_3)_3Br^-$
FS150	$C_8F_{17}SO_2NH(CH_2)_3N^+(CH_3)_3I^-$
<i>Coupling agents</i>	
10S	$[C_{10}H_{21}(CH_3)_2N(CH_2)_3Si(OCH_3)_3]^+Cl^-$
12S	$[C_{12}H_{25}(CH_3)_2N(CH_2)_3Si(OCH_3)_3]^+Cl^-$
14S	$[C_{14}H_{29}(CH_3)_2N(CH_2)_3Si(OCH_3)_3]^+Cl^-$
16S	$[C_{16}H_{33}(CH_3)_2N(CH_2)_3Si(OCH_3)_3]^+Cl^-$
18S	$[C_{18}H_{37}(CH_3)_2N(CH_2)_3Si(OCH_3)_3]^+Cl^-$
Edran	
FC805	
<i>Resins</i>	
SR2411	Silicone
Versamid 940	Polyamide
Torayneecce	Polyimide

the following formula is obtained.

$$1 + \cos \alpha = \frac{2\{(\gamma_s^d \gamma_L^d)^{1/2} + (\gamma_s^p \gamma_L^p)^{1/2}\}}{\gamma_L} \quad (25)$$

Equation (25) enables to derive (γ_s^d, γ_s^p) from measured α values for several liquids with known (γ_L^d, γ_L^p) values. Test liquids used are listed in Table II, together with their (γ_L^d, γ_L^p) values.^{18,23} α values were measured for the substrates in Table I using a contact angle meter.¹¹ Measured α values are shown in Table III. By substituting these α and (γ_L^d, γ_L^p) values into Eq. (25) and using the least square method, (γ_s^d, γ_s^p) values were derived for each substrate in Table I. The results are listed in Table IV and shown in Figure 4. Dotted

TABLE II
Liquids used for contact angle measurements (Refs. 18 and 23).

Liquids	(erg/cm ²)	
	γ^d_L	γ^p_L
Water	22.0	50.2
Glycerol	34.0	30.0
Formamide	32.3	26.0
di-Iodomethane	48.5	2.3
α -Bromonaphthalene	44.6	0.0
<i>n</i> -Hexadecane	27.6	0.0
<i>n</i> -Tetradecane	26.7	0.0
<i>n</i> -Dodecane	25.4	0.0
<i>n</i> -Decane	23.9	0.0
<i>n</i> -Octane	21.8	0.0
<i>n</i> -Hexane	18.4	0.0

lines in Figure 4, which start at the “Glass” point and end at the “FS150” and “12S” points, connect measured (γ^d_s, γ^p_s) values for different concentrations *C* of FS150 and 12S aqueous solutions used for the substrate surface treatments respectively. In the case of FS150 treatments, *C* changes from 3.9×10^{-4} mol/l at the “FS150” point to 0 at the “Glass” point. As is shown in Figure 4, FS150 richer solutions make the substrate dispersive surface energy smaller. In the case of 12S treatments, *C* changes from 1.2×10^{-3} mol/l at the “12S” point to 0 at the “Glass” point. In this case, 12S richer solutions make the substrate polar surface energy smaller. These *C*-dependences of (γ^d_s, γ^p_s) were reported in a previous paper¹¹ in detail. In Figure 4, the calculated conditions for producing the MBBA homeotropic orientation (See Figure 2) are also shown as a shadowed region.

The actual orientation angles θ_0 of MBBA at the substrate surfaces were measured by the magneto-null capacitance method on the monitoring In₂O₃ electrodes, and confirmed by conoscopic observations on the bare glass area. Measurements were performed for the substrate surfaces in Table I. The results are summarized in Table IV and shown in Figure 4. In Figure 4, circles represent the MBBA homeotropic orientation ($\theta_0 = 0^\circ$) and crosses represent the MBBA non-homeotropic orientations ($\theta_0 \neq 0^\circ$). As clearly shown in Figure 4, calculated and measured results on the MBBA interfacial orientation angles are in fairly good agreement.

B_θ derivations for MBBA As was described in Section 2, *B_θ* for MBBA can be calculated from measured (γ^d_s, γ^p_s) values and Eqs. (20) and (22). (γ^d_s, γ^p_s) values were measured for the surfaces of substrates covered with silane coupling agent *n*S layers (*n* = 10, 12, 14, 16, 18). The (γ^d_s, γ^p_s) values and calculated *B_θ* values for MBBA are listed in Table V. On the other hand, *B_θ* can be derived from critical field strength measurements for the Fredericksz transi-

TABLE III
Measured contact angles.

Liquids	Surfactants				Coupling agents						Resins			
	Glass	6Br	8Br	FS150	10S	12S	14S	16S	18S	Edran	FC805	SR2411	Versamid 940	Toray-necce
Water	3.5	31.1	56.4	71.3	80.9	84.7	82.2	83.9	84.0	86.5	97.3	106.8	104.6	70.4
Glycerol	9.1	38.4	52.5	83.6	70.6	73.3	76.2	74.7	77.4	84.1	75.7	99.4	98.5	58.6
Formamide	3.5	19.9	29.5	53.4	61.1	57.4	64.2	67.2	70.3	73.2	69.1	99.5	94.7	45.5
di-Iodomethane	46.8	40.4	52.6	98.5	52.5	51.9	54.2	53.0	55.9	54.3	77.6	88.2	70.1	38.4
α -Bromonaphthalene	10.7	9.3	25.1	88.9	30.8	35.6	40.9	34.5	34.1	32.0	90.0	67.8	27.4	17.6
<i>n</i> -Hexadecane	9.6	5.6	14.8	76.3		~0		~0		4.1	66.2			
<i>n</i> -Tetradecane	~0	4.0	4.3	74.8						8.6	62.2	30.8	10.8	6.2
<i>n</i> -Dodecane		~0	~0	70.4						5.9	59.3	24.1	4.1	8.3
<i>n</i> -Decane				67.1							47.5	15.0	5.7	6.9
<i>n</i> -Octane				60.9							26.0	~0	~0	~0
<i>n</i> -Hexane				44.4							7.2			

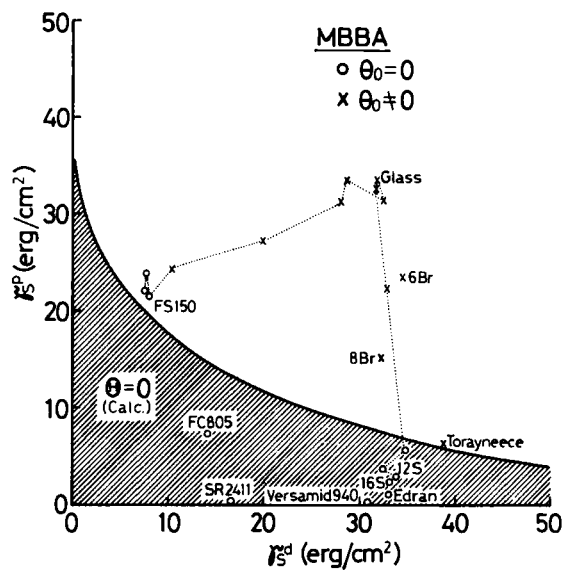


FIGURE 4 Measured substrate surface energy components (γ_s^d , γ_s^p) and MBBA orientation angles θ_0 .

TABLE IV
Derived substrate surface energy components and measured MBBA orientation angles.

	γ_s^d	γ_s^p	θ_0 (MBBA)
	(erg/cm ²)		(deg)
No coating			
Glass	32.0	33.6	90
Surfactants			
6Br(C ₆ H ₁₃ ⁺ , Cation)	34.6	23.7	~75
8Br(C ₈ H ₁₇ ⁺ , —)	32.4	15.2	~75
FS150(C ₈ F ₁₇ ⁺ , —)	7.7	22.2	0
Coupling agents			
10S(C ₁₀ H ₂₁ ⁺ , Silane)	34.0	3.5	0
12S(C ₁₂ H ₂₅ ⁺ , —)	33.9	3.0	0
14S(C ₁₄ H ₂₉ ⁺ , —)	31.1	3.3	0
16S(C ₁₆ H ₃₃ ⁺ , —)	33.2	2.4	0
18S(C ₁₈ H ₃₇ ⁺ , —)	32.2	2.2	0
Edran (C ₁₇ H ₃₅ ⁺ , Chrome complex)	33.1	1.1	0
FC805(C ₈ F ₁₇ ⁺ , —)	14.2	7.4	0
Resins			
SR2411 (Silicone)	16.6	0.4	0
Versamid 940 (Polyamide)	30.8	0.2	0
Torayneecce (Polyimide)	38.9	6.5	90

TABLE V
Derived substrate surface energy components and calculated and measured anchoring strength coefficients for MBBA.

	γ_s^d	γ_s^p	$B_\theta (\times 10^{-2})$	
			Calculated	Measured
10S(C ₁₀ H ₂₁)	34.9 ± 2.4	2.5 ± 0.6	3.4 ± 1.0	1.6 ± 0.2
12S(C ₁₂ H ₂₅)	34.6 ± 0.6	4.2 ± 0.2	2.0 ± 0.2	2.1 ± 0.9
14S(C ₁₄ H ₂₉)	34.2 ± 1.1	1.9 ± .02	4.1 ± 0.4	3.2 ± 0.8
16S(C ₁₆ H ₃₃)	34.6 ± 1.9	2.2 ± 0.5	3.7 ± 0.7	3.6 ± 0.7
18S(C ₁₈ H ₃₇)	32.9 ± 2.2	1.1 ± 0.4	5.4 ± 0.9	1.2 ± 0.6

(erg/cm²)

tion.¹⁴ The B_θ values measured by this method were previously reported¹¹ and are also listed in Table V. The calculated and the measured B_θ values agree each other within an order of magnitude, as shown in Figure 5.

4 DISCUSSION

As is clearly seen in the calculated and measured results, in Figure 4, the LC interfacial orientations are determined by the competition between polar and

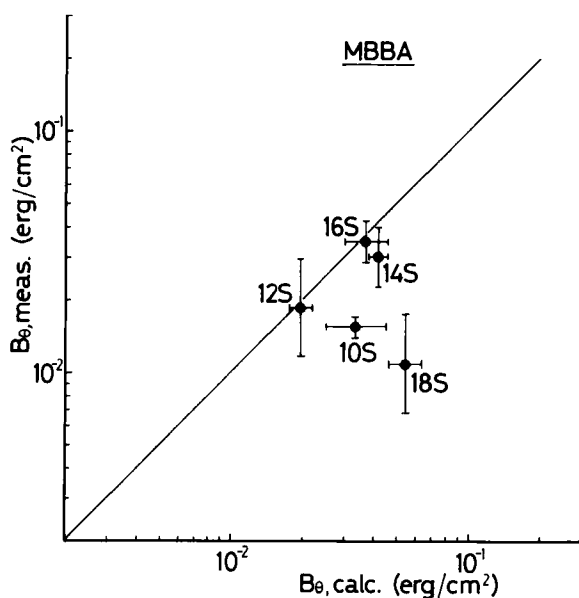


FIGURE 5 Relationships between calculated and measured anchoring strength coefficients B_θ for MBBA on substrates with nS layers.

dispersive interactions at the LC-substrate interface. In this section, discussions are made on the substrate surface energy compositions shown in Table IV, which are characteristic to the surface layer materials. The bare glass surface has rather large surface energy, $(\gamma_s^d, \gamma_s^p) = (32.0, 33.6)$. On such a substrate surface, MBBA molecules tend to align parallel to the substrate surface. In order to make MBBA molecules align homeotropically on glass substrates, it is necessary to reduce either polar or dispersive surface energy components of glass substrates. Organic layers are considered to screen the surface electrostatic field of glass substrates and reduce their polar surface energies. Obtained polar surface energies are rather large for cationic surfactants (6Br, 8Br, FS150) compared with those for coupling agents (10S ~ 18S, Edran, FC805). The rather large γ_s^d values for 6Br and 8Br are considered to be caused by their ionic characteristics and comparatively short alkyl chains insufficient to screen the surface potential. In addition, in the FS150 case, its polar $\text{—SO}_2\text{NH—}$ group is considered to play some roles to make γ_s^p rather large. On the other hand, the coupling agent layers show rather small γ_s^p values, which are thought to be produced by their chemisorption characteristics in such a manner as changing polar silanol groups on glass surfaces into siloxane bondings. For both the surfactant and the coupling agent layers, a tendency can be found that γ_s^p decreases as the alkyl chain length becomes longer. This will be an evidence of the above-mentioned screening effect and explains the empirical condition that comparatively long alkyl chains are needed for surfactants to produce the LC homeotropic orientation. Another evidence of the screening effect can be found in the C -dependence of γ_s^p for the substrates treated with 12S aqueous solutions, which was shown in Figure 4. If 12S richer solutions are used for surface treatments, 12S molecules are considered to be deposited with higher density on glass substrates. Such a 12S high density layer will screen the glass surface potential more effectively than a lower density layer. This will be the reason why 12S richer solutions make the substrate polar surface energy smaller. Compared with these γ_s^p reducing materials, FS150 is characterized by its small γ_s^d . This γ_s^d reducing effect is thought to be caused by the FS150 perfluorocarbon chain, which is well known to exhibit a small γ_s^d value. The C -dependence of γ_s^d for the substrates treated with FS150 aqueous solutions, shown in Figure 4, clearly exhibits that the FS150 layer with higher density produces smaller γ_s^d value. The small γ_s^d value caused by perfluorocarbon chains is also found for a coupling agent FC805. The γ_s^d values for surfactants and coupling agents with hydrocarbon chains are almost same. This is characteristic of the terminal —CH_3 group. The extremely small γ_s^p values obtained by the resins are considered to be the result of their rather thick layers, which were formed by the spinner coating method. The Toraynecce layer shows somewhat large γ_s^p value compared with the other resins. This is considered to be characteristic of the polyimide imino group =NH .

5 SUMMARY

The present study shows that the LC substrate interfacial orientation conditions are determined by polar and nonpolar surface energies for both LCs and substrates. For MBBA, the homeotropic orientation is expected on substrates with either small polar surface energies or small dispersive surface energies. Small polar energy surfaces are produced by screening the surface electrostatic field of glass substrates with organic layers. For this screening effect, the organic materials are desired to have no polar groups. Organic materials with perfluorocarbon chains are effective to produce small dispersive energy surfaces, where MBBA aligns homeotropically. For the anchoring strengths at the interfaces, calculations and measurements show that stronger anchoring conditions are obtained for MBBA on substrates with smaller polar and dispersive surface energies.

When LC surface energy components including their anisotropies are known, their interfacial orientation angles and anchoring strength coefficients can be estimated from substrate surface energy measurements. This provides an effective means for preparing pertinent surface-treated substrates for LC devices. In order to discuss the present results in further detail and put them more widely to practical use, the surface energy anisotropy measurements for various LC materials are required.

Acknowledgments

The author is grateful to Dr. F. Saito for encouragement and invaluable advice, and to T. Ueno, F. Ogawa and C. Tani for helpful discussions.

References

1. P. Chatelain, *Bull. Soc. Fr. Mineral. Cristallogr.*, **66**, 105 (1943).
2. J. L. Janning, *Appl. Phys. Lett.*, **21**, 173 (1973).
3. E. Guyon, P. Pieranski and M. Boix, *Lett. Appl. Eng. Sci.*, **1**, 19 (1973).
4. J. E. Proust, L. Ter-Minassian-Saraga and E. Guyon, *Solid State Commun.*, **11**, 1227 (1972).
5. F. J. Kahn, *Appl. Phys. Lett.*, **22**, 386 (1973).
6. D. W. Berreman, *Phys. Rev. Lett.*, **28**, 1683 (1972); *Mol. Cryst. Liq. Cryst.*, **23**, 215 (1973).
7. L. T. Creagh and A. R. Kmetz, *Mol. Cryst.*, **24**, 59 (1973).
8. F. J. Kahn, G. N. Taylor and H. Schonhorn, *Proc. IEEE*, **61**, 823 (1973).
9. I. Haller, *Appl. Phys. Lett.*, **24**, 349 (1974).
10. E. Perez, J. E. Proust and L. Ter-Minassian-Saraga, *Mol. Cryst. Liq. Cryst.*, **42**, 167 (1977).
11. S. Naemura, to be published in *J. Appl. Phys.*
12. G. Ryschenkow and M. Kleman, *J. Chem. Phys.*, **64**, 404 (1976).
13. G. Porte, *J. de Phys.*, **37**, 1245 (1976).
14. S. Naemura, *Appl. Phys. Lett.*, **33**, 1 (1978).
15. S. Naemura, *J. de Phys.*, **C3-40**, C3-514 (1979).
16. J. Nehring, A. R. Kmetz and T. J. Scheffer, *J. Appl. Phys.*, **47**, 850 (1976).
17. C. Tani, F. Ogawa, S. Naemura, T. Ueno, F. Saito and O. Kogure, *Proc. SID*, **21**, 71 (1980).
18. F. M. Fowkes, *Adv. Chem. Series*, **43**, 99 (1964).

19. J. D. Parsons, *Mol. Cryst. Liq. Cryst.*, **31**, 79 (1975).
20. L. A. Girifalco and R. J. Good, *J. Phys. Chem.*, **61**, 904 (1957).
21. J. D. Parsons, *J. de Phys.*, **37**, 1187 (1976).
22. E. Perez, J. E. Proust and L. Ter-Minassian-Saraga, *Adhesion 2* (Applied Science Publishers Ltd., England), Chap. 2, pp. 23-34.
23. J. R. Dann, *J. Colloid Interface Sci.*, **32**, 302 (1970).